Available online at www.sciencedirect.com
ScienceDirect
Microporous and Mesoporous Materials 108 (2008) 237–246
MICROPOROUS AND MESOPOROUS MATERIALS
www.elsevier.com/locate/micromeso

Photoluminescence behavior of Eu^{3+} ion doped into γ- and α-alumina systems prepared by combustion, ceramic and Pechini methods

M.A.F. Monteiro [a], H.F. Brito [a,*], M.C.F.C.M. Felinto [b], G.E.S. Brito [c], E.E.S. Teotonio [d], F.M. Vichi [a], R. Stefani [a]

[a] Departamento de Química Fundamental – Instituto de Química da Universidade de São Paulo, 05508-900 São Paulo, SP, Brazil
[b] Instituto de Pesquisas Energéticas e Nucleares Av Prof Lineu Prestes 2242 Cidade Universitária, CEP 05508-000 São Paulo, SP, Brazil
[c] Instituto de Física, Universidade de São Paulo, Cidade Universitária, CEP 05508-970 São Paulo, SP, Brazil
[d] Departamento de Química, Universidade Federal de Goiás, Campus Catalão, CEP 75704- 020, Catalão-GO, Brazil

Received 13 October 2006; received in revised form 21 March 2007; accepted 27 March 2007
Available online 29 April 2007

Abstract

Al_2O_3:Eu^{3+}(1%) samples were prepared by combustion, ceramic, and Pechini methods annealed from 400 to 1400 °C. XRD patterns indicate that samples heated up to 1000 °C present disordered character of activated alumina (γ-Al_2O_3). However, α-Al_2O_3 phase showed high crystallinity and thermostability at 1200–1400 °C. The sample characterizations were also carried out by means of infrared spectroscopy (IR), scanning electron microscopy (SEM) and specific surface areas analysis (BET method). Excitation spectra of Al_2O_3:Eu^{3+} samples present broaden bands attributed to defects of Al_2O_3 matrices and to LMCT state of $O \rightarrow Eu^{3+}$, however, the narrow bands are assigned to $^7F_0 \rightarrow {}^5D_J$,$^5H_J$ and ^5L_J transitions of Eu^{3+} ion. Emission spectra of samples calcined up to 1000 °C show broaden bands for $^5D_0 \rightarrow {}^7F_J$ transitions of Eu^{3+} ion suggesting that the rare earth ion is in different symmetry sites showed by inhomogeneous line broadening of bands, confirming the predominance of the γ-alumina phase. For all samples heated from 1200 to 1400 °C the spectra exhibit narrow $^5D_0 \rightarrow {}^7F_J$ transitions of Eu^{3+} ion indicating the conversion of γ to α-Al_2O_3 phases, a high intensity narrow peak around 695 nm assigned to *R* lines of Cr^{3+} ion is shown. Al_2O_3:Eu^{3+} heated up to 1100 °C presents an increase in the Ω_2 intensity parameter with the increase of temperatures enhancing the covalent character of metal–donor interaction. The disordered structural systems present the highest values of emission quantum efficiencies (η). CIE coordinates of Al_2O_3:Eu^{3+} are also discussed.

Keywords: Europium; Alumina; Luminescence; Combustion; Ceramic; Pechini methods

1. Introduction

The luminescence properties of rare earth (RE) ions in different host matrices have been extensively studied for several years [1–3]. The physical and chemical properties of RE ions doped into the host result in an improvement of its structural, electronic and optical properties, which make these materials useful for several applications, such as: laser materials, optical amplifiers, phosphors, photocatalysts etc. [3–5]. Due to the low dopant concentration, optical spectroscopy of RE ions is among the very few tools sensitive enough to be used as local luminescence probes [6].

Among the trivalent rare earth ions (RE^{3+}) that present characteristic f–f intraconfigurational emission narrow lines, the europium ion is a potential candidate to be used as luminescent materials due to its exceptional spectroscopic properties [1,2]. The Eu^{3+} ion has a great advantage because it exhibits strong red monochromatic emission color and it has also been considerably used as efficient luminescent probe due to [7]: (a) the excited $^5D_0$ state is well separated (~12,000 cm^{-1}) from ground $^7F_{0-6}$ states;

* Corresponding author. Tel.: +55 11 3091 3708; fax: +55 11 3815 5579.
E-mail address: hefbrito@iq.usp.br (H.F. Brito).

1387-1811/$ - see front matter © 2007 Elsevier Inc. All rights reserved.
doi:10.1016/j.micromeso.2007.03.045

(b) the emitter $^5D_0$ level and the ground $^7F_0$ state are non-degenerated, thus the $^5D_0 \rightarrow {}^7F_0$ transition displays a single peak when the Eu^{3+} ion occupies identical sites of symmetry of the type C_s, C_n or C_{nv}, which provides information on the eventual existence of more than one site of symmetry occupied by rare earth ion; (c) long luminescence decay time for the emitter $^5D_0$ level (milliseconds); (d) exceptionally large Stokes' shift when the emission spectra are obtained through direct excitation of the $^5L_6$ level (~394 nm) of the Eu^{3+} ion and (e) the radiative rate of the $^5D_0 \rightarrow {}^7F_1$ transition is formally insensitive to the crystal field environment and consequently can be used as a reference transition. The ligand-to-metal charge transfer state (LMCT) of Eu^{3+} ion corresponds to reduction $4f^6 \rightarrow 4f^7L^{-1}$, where the Eu^{3+} ion tends to reduce in order to obtain the half-filled stable shell configuration [7,8].

Nowadays, alumina has been used as catalysts, catalyst supports, adsorbent and ceramic materials owing to its inertness, good mechanical properties, stability under most reaction conditions, high surface area and low cost [9,10]. In particular, γ-Al_2O_3 is extensively used as a support for industrial catalyst. The γ-alumina phase is stable up to 900 °C but by heating above this temperature converts it into α-alumina through a series of polymorphic transformations $\gamma \rightarrow \delta \rightarrow \theta \rightarrow \alpha$-alumina [11]. The phase transformation from γ- to α-alumina decreases the surface area that causes serious problems for application as catalysts.

The stable phase, α-Al_2O_3 (corundum), is an optical material with a significant technological importance due to high optical transparency in the spectral range from ultraviolet to near-infrared, excellent mechanical properties, and good chemical stability [12]. The Al^{3+} ions in the alumina lattice are easily replaced by iron-group 3d ions, for example, Cr^{3+} ion in ruby gemstone (α-Al_2O_3:Cr^{3+}), however, the incorporation of group 4f ions, RE^{3+} ions with larger size, in alumina host is difficult to be reached by traditional methods [11]. The incorporation of rare earth ions to alumina generally enhances its thermal stability of γ-Al_2O_3 phase and the europium ion is particularly suitable for the photoluminescence investigation of different phases when doped into alumina matrices [12–19].

The goal of this work is to use the Eu^{3+} ion doped in Al_2O_3 host as local photoluminescence probes and to investigate the behavior of this ion in different alumina phases when prepared by three different methods, such as: Pechini [20] and combustion [21] as alternative methods, in milder experimental conditions than the solid state reaction (ceramic method) [22]. Luminescent behavior of Eu^{3+} ion in this matrix was investigated based on 4f–4f intraconfigurational transitions. Experimental quantum efficiencies (η) for the emitting $^5D_0$ level of europium ion were determined and discussed.

2. Experimental procedure

The Al_2O_3 matrix doped with Eu^{3+} ion was obtained by the following preparation processes: (a) *Ceramic method* – An aqueous solution containing stoichiometric amounts of $Al(NO_3)_3 \cdot 9H_2O$ (Synth) together with 1 mol% dopant concentration of Eu^{3+} added as $Eu(NO_3)_3 \cdot 6H_2O$ (prepared from Eu_2O_3, Aldrich, 99.9%) were evaporated and throughly mixed and triturated. The mixtures were heated in air atmosphere at 800, 900, 1000, 1100, 1200 and 1400 °C in alumina crucibles during 8 h; (b) *Pechini method* – The stoichiometric quantities of $Al(NO_3)_3 \cdot 9H_2O$ precursor and 1 mol% of $Eu(NO_3)_3 6H_2O$ were dissolved in deionized water. To this solution, preheated at 70 °C, citric acid was added in a weight ratio of 3.6:1 (citric acid:ethylene glycol) under stirring. Then, this mixture was heated at 110 °C, and the formation of brown transparent glassy polymeric resin was observed. After that, the resin was heated at 300 °C for 2 h, resulting in a fluffy black mass, which was grounded to get a fine powder. Finally, this material was calcinated at different temperatures (900, 1100, 1200 and 1400 °C) during 4 h, resulting in Al_2O_3:Eu^{3+} system. These samples prepared by Pechini process began been heated at 900 °C to prevent the carbon contamination observed when heated up to 800 °C, presenting gray color arising from the organic precursors (citric acid and ethylene glycol). When these powder samples are heated at 900 °C, the white color indicates the absence of carbon and (c) *Combustion method* – Similar molar quantities of reagents to traditional ceramic method were used. Urea (CH_4N_2O) in 2.5 mol% was used as fuel, which was added to mixture of rare earth (1 mol%) and aluminum nitrates dissolved in deionized water. Resultant solutions were heated at 300 °C (3 °C/min) on a hot plate to dehydrate and decompose. Then, in a few seconds, the mixture ignites, leading to smooth deflagration with enormous swelling, producing a white foam. In this chemical reaction, O_2, N_2, NO_2, NH_3, H_2O and CO_2 gases are released. The voluminous and foamy solids were heated at 400, 700, 800, 900, 1000, 1100, 1200 and 1400 °C for 4 h, yielding a white powder of Al_2O_3:Eu^{3+} system.

Undoped alumina (Al_2O_3) was also obtained by the same three preparation methods reported above, in order to compare the alumina phases at different annealing temperatures.

The different phases of alumina doped with Eu^{3+} ions were determined by X-ray diffraction patterns recorded on a Phillips diffractometer model X'Pert-MPD using a Cu Kα radiation (40 kV and 40 mA) in the interval of 2–70° (2θ) and 1 s of pass time, using the powder XRD method. The average crystallite particle size of the samples was determined using the Scherrer's formula [23].

The infrared absorption spectra were recorded in KBr pellets on a Bomen Model MB-100 spectrophotometer in the spectral range of 4000–400 cm^{-1}. Scanning electron microscopy (JEOL JSM 840 A) was used to visualize the morphology of the final alumina powders. The pore structures and the specific surface areas of the samples were determined by N_2 adsorption/desorption isotherm analysis using a Quantachrome Nova 1000e surface area and pore size analyzer. The surface areas were calculated using the BET method.

Photoluminescence measurements were performed with a spectrofluorometer (SPEXFluorolog 2) with a double grating 0.22 m monochromator (SPEX 1680) and a 450 W Xenon lamp as the excitation source. To eliminate the second-order diffraction of the source radiation, a cut off filter was used in the measurements. All excitation and emission spectra were recorded at room (298 K) and liquid nitrogen (77 K) temperatures and collected at an angle of 22.5° (front face) using a detector mode correction. The luminescence decay curves of the emitting levels were recorded at 300 K, using a phosphorimeter SPEX 1934D accessory coupled to the spectrofluorometer. The signals were detected by a water-cooled Hamamatsu R928 photomultiplier and processed by a DM3000F SPEX system.

3. Results and discussion

3.1. Characterization

Fig. 1a shows the X-ray diffraction patterns of the Al_2O_3:Eu^{3+} samples prepared by combustion method as synthesized, and treated at different temperatures from 400 to 1400 °C. The XRD patterns present no Bragg reflections for the samples as-synthesized and thermally treated from 400 to 700 °C confirming the amorphous character of alumina samples, however at 800 and 900 °C broaden peaks arise due to structural disorder host lattice corresponding to the cubic phase with the predominance of γ-Al_2O_3 phase for this system (Fig. 1a). For the samples annealed at 1100, 1200 and 1400 °C, the XRD patterns present well-defined reflections indicating a stable crystalline hexagonal structure of α-Al_2O_3 phase.

When the XRD data of doped system (Fig. 1a) are compared with the undoped alumina (Fig. 1b) it is observed an effective action of the doping in the alumina matrices, which prolongs the γ-Al_2O_3 phase up to 900 °C. However, the presence of α-Al_2O_3 phase for the undoped alumina at 900 °C is confirmed by the diffraction pattern peaks indicated by presence of highly crystalline α-alumina phase (Fig. 1b).

The XRD patterns for the Al_2O_3:Eu^{3+} (1%) samples obtained by ceramic and Pechini methods at 900 °C also exhibited very similar profiles to those prepared by combustion at the same temperature, corroborating with the prolonging of the γ-Al_2O_3 phase by the doping with rare earth ion.

The values of average particle size [23] of Al_2O_3:Eu^{3+} samples prepared by combustion, ceramic and Pechini methods (at 900 °C) are around 40 Å. The dopant ion occupies vacancy sites of alumina lattice that hinder the

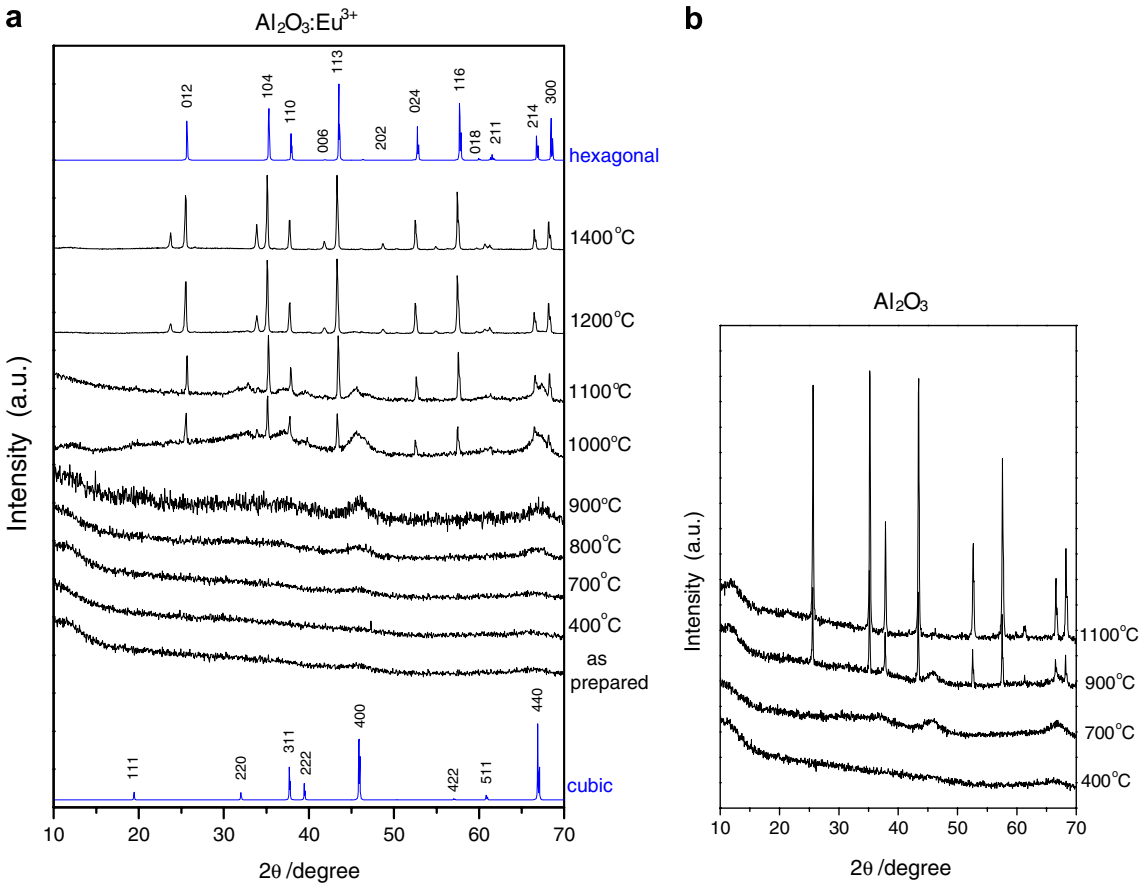

Fig. 1. XRD patterns of samples prepared by combustion method of (a) doped alumina as synthesized and thermally treated from 400 to 1400 °C and (b) undoped alumina heated at 400–1100 °C.

atomic mobility which can increase crystallite size by a lattice diffusion process. These powder samples heated below 1100 °C show a cubic structure and are constituted of nanodomains.

The IR spectra of all undoped and doped alumina samples heated up to 900 °C presented broad stretching bands in the region of 3500–3200 cm^{-1} assigned to the ν_s and ν_{as}OH stretchings and δHOH-bending at 1630–1600 cm^{-1} [24]. However, when the alumina samples are treated at 1100, 1200 and 1400 °C, the broad stretching bands attributed to the water molecules vanished indicating that these systems are anhydrous.

In general, the infrared spectra of Al_2O_3:Eu^{3+} show stretching frequencies (870–750 cm^{-1}) related to condensed and/or isolated tetrahedral [AlO_4] groups, indicating the presence of γ-alumina phase. It was also observed the existence of bands in the spectral range of 650–500 cm^{-1} in lower energies attributed to stretching frequencies of octahedral [AlO_6] groups from stable α-alumina phase. These frequencies are only observed for the system treated above 1100 °C suggesting the presence of α-Al_2O_3 phase indicating that Eu^{3+} ion stabilizes the γ-Al_2O_3 phase up to 900 °C, corroborating with their XRD patterns data [25–27].

The scanning electronic micrograph of Al_2O_3:Eu^{3+} samples obtained by ceramic, combustion and Pechini methods and thermally treated at 900 °C are shown in Fig. 2a–c, respectively. The micrographs of alumina prepared by ceramic method show more homogeneous morphology and lower size of particle agglomerates than those prepared by Pechini and combustion processes. Particularly the material obtained by Pechini method has the largest size of particle agglomerates, however it also presents more homogeneous morphology when compared with that synthesized by Pechini method in accordance to the literature [28].

For the system prepared by combustion method it was observed that the agglomerated particles are the largest observed when prepared by other methods. This behavior could be attributed to the strong heat involved in the combustion reaction, when urea is considered the combustion fuel in this process. This fuel forms an intermediate stable phase capable of keeping the heat, increasing the particle size [29,30]. SEM micrographs of alumina prepared by combustion process treated at 400, 700 and 900 °C presented larger particle sizes for the system calcined at 400 °C, but with similar aspects of sharp and regular shaped particles.

Table 1
Values of BET surface area (in m^2/g) of Al_2O_3:Eu^{3+} samples prepared by combustion, Pechini and ceramic methods treated at different temperatures

Temperature (°C)	Combustion	Pechini	Ceramic
400	208.1	–	–
700	224.4	–	–
900	134.4	79.3	52.1
1000	83.8	58.7	23.2
1200	7.0	23.8	4.8
1400	3.2	4.3	1.4

The specific surface areas of the Al_2O_3:Eu^{3+} samples prepared by the combustion, Pechini and ceramic processes and treated at different temperatures are presented in Table 1. For the materials obtained by the combustion method, the surface area increases from 208.1 $m^2\,g^{-1}$ at 400 °C to 224.4 $m^2\,g^{-1}$ at 700 °C, due to the crystallization of the γ-alumina phase, consisting of ultra-fine particles [31]. When the temperature is increased to 900 °C some particle sintering occurs and the BET surface area drops from 83.8 to 7.0 $m^2\,g^{-1}$. In all prepared samples, an abrupt decrease in the BET surface area is observed between 1000 and 1200 °C. This is consistent with the phase transition from α- to γ-alumina, which occurs at around 1100 °C, corroborated by XRD patterns data for the samples heated at 1200 °C (Fig. 1a) confirming the formation of α-alumina phase.

3.2. Photoluminescent study

The excitation spectra of Al_2O_3:Eu^{3+} samples prepared by combustion, ceramic and Pechini methods at different temperatures were recorded in the spectral range from 250 to 590 nm under emission around 612 nm and are shown in Fig. 3. It is noted a broad intense band in the range of 250–350 nm that is associated to alumina intrinsic luminescence and the ligand-to-metal charge-transfer states from

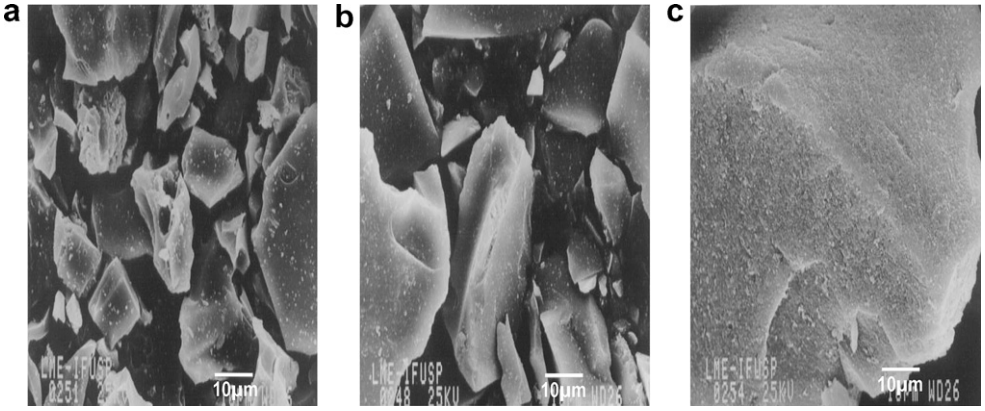

Fig. 2. SEM micrographs of Al_2O_3:Eu^{3+} samples prepared by methods (at 900 °C): (a) ceramic, (b) combustion and (c) Pechini.

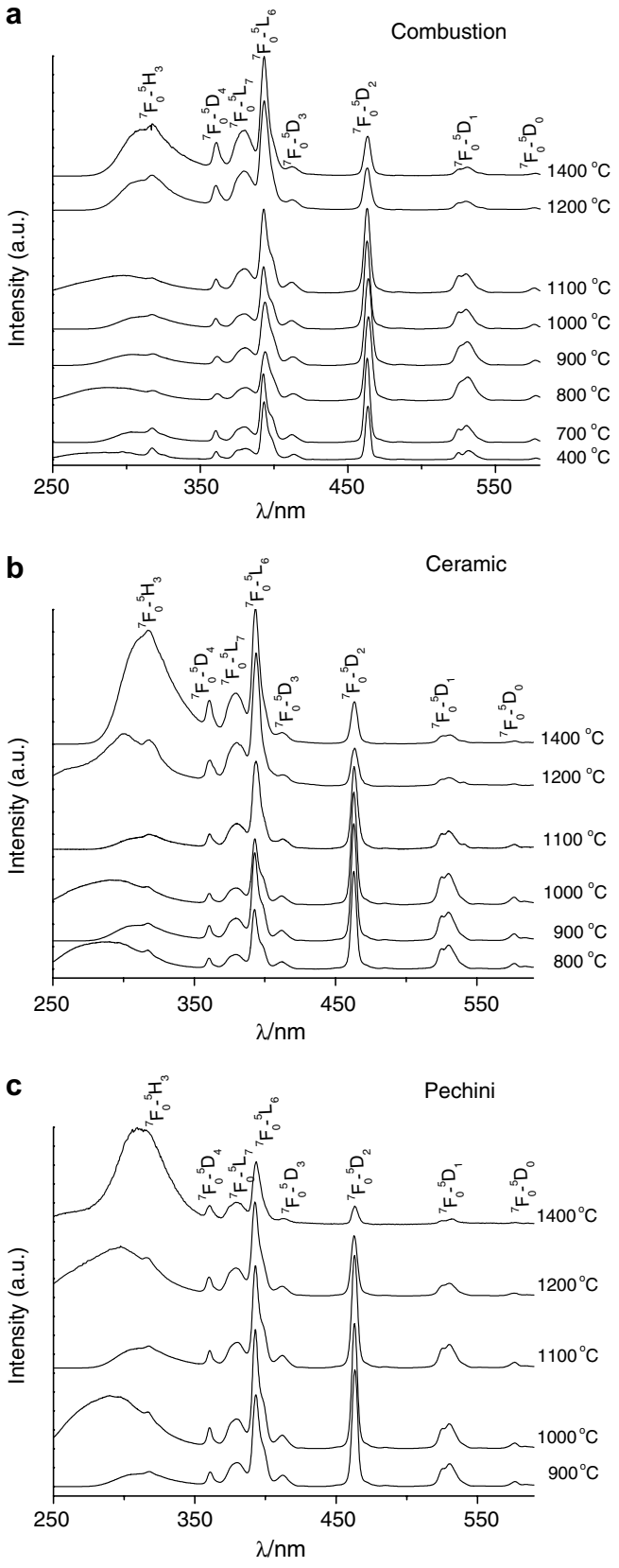

Fig. 3. Excitation spectra of Al_2O_3:Eu^{3+} samples prepared by methods: (a) combustion (400–1400 °C) (b) ceramic (800–1400 °C) and (c) Pechini (900–1400 °C).

the O → Eu^{3+} transitions (LMCT) at around 305 nm. It is also observed in Fig. 3a–c that the broaden bands are enveloped with the peaks at around 296, 305 and 315 nm, corresponding to the $^7F_0 \rightarrow {}^5F_{2,4}$ and $^5H_3$ transitions from the Eu^{3+} ion. As it can be seen, the spectral data also exhibit bands arising from the $^7F_0 \rightarrow {}^5L_6$, $^7F_0 \rightarrow {}^5D_J$ ($J = 0$–3) transitions of the rare earth ion [27–30]. The samples treated up to 1000 °C exhibit similar spectral profiles, suggesting the presence of disordered structural phase. However, the excitation spectra of the samples heated at 1100, 1200 and 1400 °C show a decrease of the intensity of the $^7F_0 \rightarrow {}^5D_2$ transition when compared to the $^7F_0 \rightarrow {}^5L_6$ transition indicating an alteration of the chemical environment around Eu^{3+} ion, suggesting the transformation of γ- to α-Al_2O_3 phases, which are corroborated by XRD patterns.

Fig. 4 presents the emission spectra for the Al_2O_3:Eu^{3+} samples prepared by combustion process after heated at 400 to 1400 °C monitoring the excitation on $^7F_0 \rightarrow {}^5L_6$ transition (394 nm) and recorded at room temperature in spectral range of 550–720 nm. These optical data exhibit the bands corresponding to $^5D_0 \rightarrow {}^7F_J$ transitions ($J = 0$, 1, 2, 3 and 4) from the Eu^{3+} ion and *R* lines arising from Cr^{3+}.

The emission spectra for the Al_2O_3:Eu^{3+} samples annealed from 400 to 1100 °C exhibit broadened bands arising from excited $^5D_0$ state to ground ^5F_J states of Eu^{3+} ion due to inhomogeneous line broadening of the transitions, suggesting that the alumina doped with europium ion presents a disordered structural character. This result also indicates the formation of the γ-alumina phase. However, increasing the temperature from 1200 to 1400 °C indicates the transformation of γ- to α-Al_2O_3 phases due to the presence of 4f → 4f transitions characteristic narrow lines assigned to $^5D_0 \rightarrow {}^7F_{0-4}$ transitions of Eu^{3+} ion (Fig. 4). When the doped alumina is prepared by combustion method it is observed that the inclusion of trivalent europium ion into α-alumina lattice presents even larger ionic radius of Eu^{3+} ion (0.947 Å) than Al^{3+} ion (0.570 Å) and inhibits the formation of α-Al_2O_3 phase bellow 1200 °C temperatures [5]. As it can be seen, in Fig. 1b the transformation of γ-to α-Al_2O_3 phase in the undoped alumina has already occurred at 900 °C.

The emission spectra of the sample treated at 1200 and 1400 °C (Fig. 4) also present high intense narrow peaks at around 662 and 693 nm and in the red region that are originated from spin forbidden transitions from excited states derived from $^2E_g(G)$ and $^2T_g(G)$ to the ground state ^4A_g from Cr^{3+} ion. These doublet states are further split by spin–orbit coupling interactions with the $^2E_g(G)$ state producing ruby R_1 (693.5 nm) and R_2 (695.0 nm) lines (inset Fig. 4) [32]. The emission ($^2E_g \rightarrow {}^4A_g$ transition) *R* lines of Cr^{3+} ions observed in bulk α-Al_2O_3:Eu^{3+} crystals may serve as an additional qualitative argument for the samples under study belonging to α-Al_2O_3 phase. Besides, these peaks indicate the occurrence of accidental Cr^{3+} impurities in the precursor of alumina matrices [11].

The emission spectra ascribed to Al_2O_3:Eu^{3+} prepared by ceramic (800–1400 °C) and Pechini (900–1400 °C)

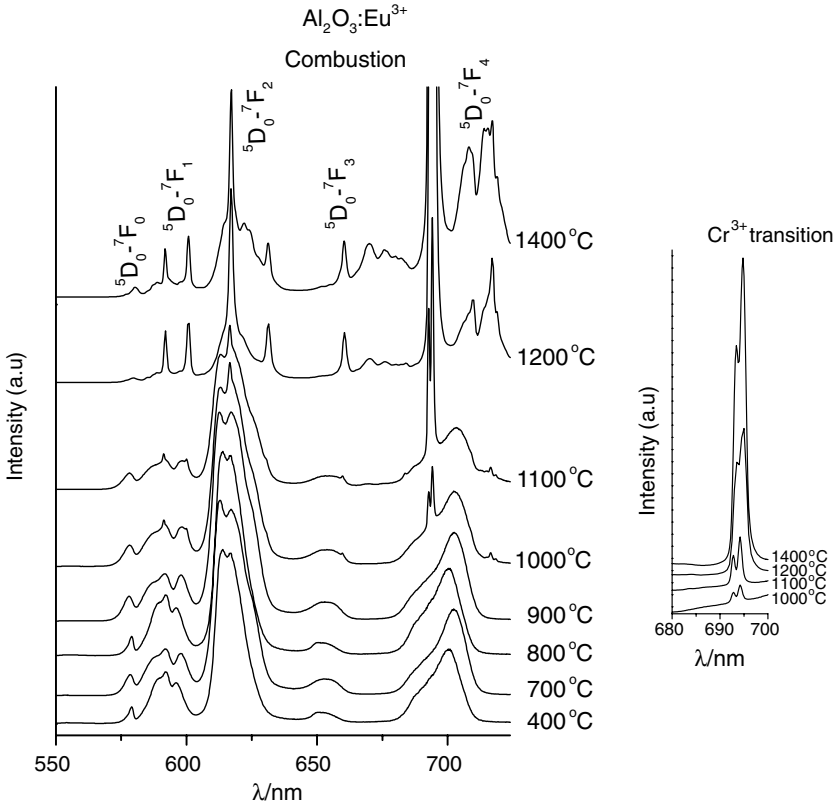

Fig. 4. Emission spectra of Al_2O_3:Eu^{3+} samples prepared by combustion method heated from 400 to 1400 °C.

processes, under excitation at 394 nm, are shown in Fig. 5. The nature of broad emission bands observed for the samples when heated at 800–1100 °C are also attributed to the inhomogeneous line broadening of the $^5D_0 \rightarrow {}^7F_{0-4}$ transitions of europium ion, indicating that the samples present disordered structural phase with the formation γ-alumina. A comparison of the emission spectral profiles of alumina treated at 1100 °C by combustion (Fig. 4), ceramic (Fig. 5a) and Pechini (Fig. 5b) methods reveal the occurrence of sharp peaks assigned to $^5D_0 \rightarrow {}^7F_{0-4}$ transitions of Eu^{3+} ion indicating the formation of α-alumina when prepared by ceramic method which differ substantially from the samples obtained by Pechini and combustion processes due to the presence of broaden bands arising from disordered structural lattice. The photoluminescence data for the Al_2O_3:Eu^{3+} samples prepared by two these different methods and treated at 1200 and 1400 °C show the sharp peaks from 4f → 4f transitions of the Eu^{3+} ion confirming the presence of α-Al_2O_3 phase. The samples prepared by ceramic and Pechini methods annealed at 1100 to 1400 °C also show the emission R lines of Cr^{3+} ions (693.5 and 695 nm) corroborating to the formation of α-Al_2O_3:Eu^{3+} phase (inset Fig. 5a and b).

Based on the luminescence decay curves for all Al_2O_3:Eu^{3+} samples prepared by three method, under excitation at 394 nm and emission at 612 nm, the lifetime values (τ_1 and τ_2) of the emitter $^5D_0$ level of the Eu^{3+} ion were determined (Table 2). These decay curves present a bi-exponential behavior, indicating that there is more than one type of chemical environment around the Eu^{3+} ion for the samples heated up to 1100 °C due to structural disordering of the systems, except for ceramic method at 1100 °C. On the other hand, the Eu^{3+} ions doped in α-Al_2O_3 obtained at 1200 and 1400 °C occupy only one position in the regular crystal lattice where there is no structural disorder and the bi-exponential values for this system are due to the presence of Cr^{3+} ion.

The standard theory of 4f–4f transition intensities gives the intensity Ω_λ parameters (where $\lambda = 2$, 4 and 6), which is the integrated coefficient of spontaneous emission (radiative) of a transition between two manifolds J and J'. These parameters contain the contributions from the forced electric dipole and dynamic coupling mechanisms. Since the radiative decay rate of the $^5D_0 \rightarrow {}^7F_1$ allowed by magnetic dipole transition is almost insensible to the crystal field environment around the trivalent europium ion, this transition can be taken as a internal standard in order to determine the radiative decay rates assigned to the $^5D_0 \rightarrow {}^7F_{2,4}$ transitions (A_{02} and A_{04}). The emission intensity, $I = \hbar\omega A\ N$, is expressed in terms of the surface under the emission curve, where $\hbar\omega$ is the transition energy, N is the population of the emitting $^5D_0$ level and the coefficient of spontaneous emission A is given by [33–35]:

$$A = \frac{4e^2\omega^3}{3\hbar c^3}\left(\frac{1}{2J+1}\right)\left[\frac{n_0(n_0^2+2)^2}{9}\right]\sum_{\lambda=2,4,6}\Omega_\lambda\left\langle {}^5D_0\left\|U^{(\lambda)}\right\|{}^7F_J\right\rangle^2, \quad (1)$$

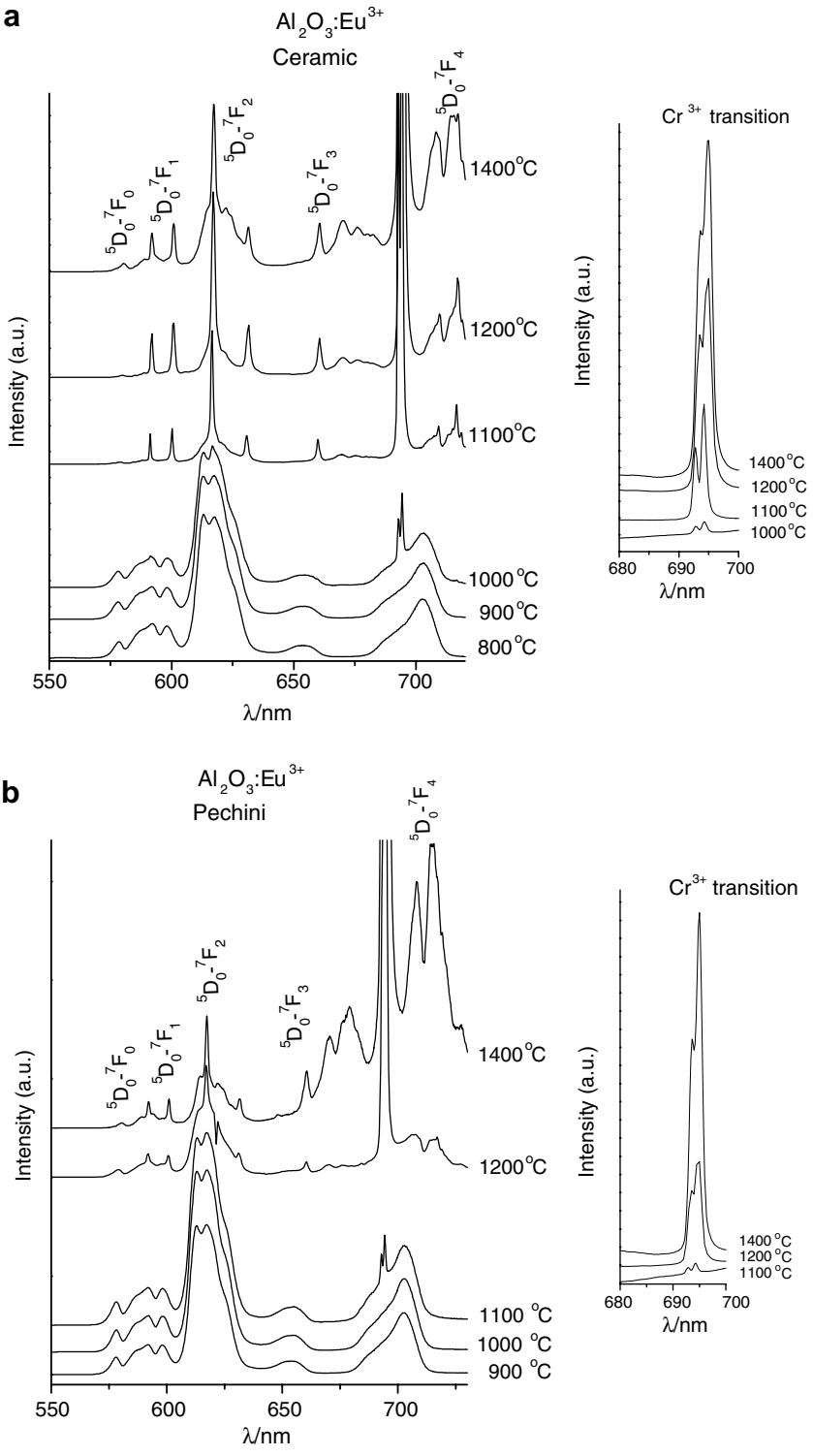

Fig. 5. Emission spectra of Al_2O_3:Eu^{3+} samples prepared by methods: (a) ceramic (800–1400 °C) and (b) Pechini (900–1400 °C).

where $\frac{n_0(n_0^2+2)^2}{9}$ is a Lorentz local field correction with refraction index $n_0 = 1.5$. The square reduced matrix elements [35] are $\langle {}^5D_0 \| U^{(2)} \| {}^7F_2 \rangle^2 = 0.0032$ and $\langle {}^5D_0 \| U^{(4)} \| {}^7F_4 \rangle^2 = 0.0023$ in Eq. (1). In this case the A values are obtained by using the relation: $A = A_{01}\Sigma_\lambda \frac{S_{0\lambda}\sigma_1}{S_{01}\sigma_\lambda}$, where $S_{0\lambda}$ is the area under the emission curve related to the ${}^5D_0 \rightarrow {}^7F_\lambda$ transitions, σ_λ is the energy barycenter of these transitions. The coefficient of spontaneous emission, A_{01} is given by the expression $A_{01} = 0.31 \times 10^{-11}(n_0)^3(v_{01})^3$, and its values are estimated to be around 50 s^{-1} [36]. The Ω_6 intensity parameter was not included in this calculation since the ${}^5D_0 \rightarrow {}^7F_6$ transition (around 850 nm) could not be observed. The lifetime (τ), non-radiative (A_{nrad}) and radiative (A_{rad}) rates are related through the following

Table 2
Experimental intensity parameters (Ω_λ), emission quantum efficiency (η), lifetimes (τ), non-radiative (A_{nrad}), radiative (A_{rad}) and total (A_{total}) rates and CIE coordinates (x, y) for the Al_2O_3:Eu^{3+} prepared by combustion, ceramic and Pechini heated at different temperatures (T)

Preparation methods (T)	A_{rad} (s^{-1})	A_{nrad} (s^{-1})	A_{total} (s^{-1})	Ω_2 (10^{-20} cm^2)	Ω_4 (10^{-20} cm^2)	τ_1 (μs)	τ_2 (μs)	η (%)	x	y
Combustion										
400 °C	569	3544	4114	6.9	8.4	308	1160	14	0.670	0.318
700 °C	563	3439	3992	11.3	12.0	299	1546	14	0.678	0.316
800 °C	880	1884	2764	18.8	18.3	446	1914	32	0.677	0.318
900 °C	590	2037	2627	12.0	12.3	477	1880	23	0.681	0.317
1000 °C	587	3154	3741	12.1	12.0	319	1651	16	0.684	0.314
1100 °C	729	2659	3388	14.0	17.8	382	1294	21	0.667	0.331
1200 °C	562	3969	4531	7.9	19.2	268	1251	12	0.674	0.317
1400 °C	679	4042	4725	9.9	23.0	255	1244	14	0.683	0.312
Ceramic										
800 °C	534	2676	3210	10.7	11.3	389	1564	17	0.680	0.317
900 °C	588	2210	2798	12.2	11.9	458	1629	21	0.679	0.317
1000 °C	618	1678	2295	12.6	13.0	587	1692	27	0.684	0.314
1100 °C	602	4130	4732	9.5	18.6	244	1577	13	0.682	0.313
1200 °C	545	3601	4146	7.5	18.8	282	1667	13	0.670	0.312
1400 °C	710	4115	4835	9.9	25.7	245	1328	15	0.665	0.326
Pechini										
900 °C	680	2366	3046	14.0	14.5	387	2176	22	0.683	0.315
1000 °C	705	1790	2495	15.2	13.8	489	2219	28	0.683	0.315
1100 °C	733	2923	3656	15.3	15.7	315	2076	20	0.665	0.331
1200 °C	638	3642	4281	11.6	16.8	111	1491	15	0.666	0.324
1400 °C	701	3543	4245	8.9	26.4	291	1237	16	0.685	0.304

equation: $A_{tot} = \frac{1}{\tau} = A_{rad} + A_{nrad}$, where the A_{rad} rate was obtained by summing up over the radiative rates A_{0J} for each $^5D_0 \rightarrow {}^7F_J$ transitions ($A_{rad} = \Sigma_J A_{0J}$). The emission quantum efficiency of the emitting $^5D_0$ level is given by

$$\eta = \frac{A_{rad}}{A_{rad} + A_{nrad}} \quad (2)$$

In Table 2 the values of the Ω_λ intensity parameters ($\lambda = 2$ and 4) are shown for the Al_2O_3:Eu^{3+} material annealed from 400 to 1400 °C. When a comparison is made among the Ω_2 parameters for these samples, it is noted that the highest value (18.0×10^{-20} cm^2) is found for the sample prepared by combustion heated at 800 °C indicating the highest hypersensitive behavior of the $^5D_0 \rightarrow {}^7F_2$ transition. Consequently, the Eu_{3+} ions, in this case, are in a higher polarizable environment than in the other alumina samples, suggesting a higher electric dipole character to the $^5D_0 \rightarrow {}^7F_2$ transition for the sample treated at 800 °C. This result indicates a moderate covalent character of the metal–donor atom interaction of Eu^{3+} ion in alumina matrix. It is also observed in Table 2 an increase of Ω_2 parameters with augment of annealed temperature for disordered phase, γ-Al_2O_3 – Combustion: from 6.9 to 14.0×10^{-20} cm^2 (400–1000 °C), except for the sample heated at 800 °C – Ceramic: from 12.2 to 12.0–12.6 $\times 10^{-20}$ cm^2 (900–1000 °C) and Pechini: from 14 to 15.3×10^{-20} cm^2 (900–1100 °C). Therefore this might suggest that the site of symmetry occupied by the Eu^{3+} ion has no character of centrosymmetric chemical environment considering that the $^5D_0 \rightarrow {}^7F_2$ transition is formally forbidden due to the electric dipole selection rule. Nevertheless, the Ω_2 values decrease as temperature increases, indicating that the Eu^{3+} ion doped in alumina is found in a different chemical environment, where the hypersensitive $^5D_0 \rightarrow {}^7F_2$ transition of europium ion corroborates with the evidence of changing from the disordered to crystalline phase (α-Al_2O_3).

The Ω_4 experimental intensity parameters were determined from the bands assigned to $^5D_0 \rightarrow {}^7F_4$ transition of Eu^{3+} ion. For the Al_2O_3:Eu^{3+} samples heated higher than 1000 °C, those bands are enveloped with emission peaks attributed to $^2E_g \rightarrow {}^4A_g$ transition arising from the Cr^{3+} ion. In order to obtain the surface under the curve of $^5D_0 \rightarrow {}^7F_4$ transition a deconvolution program was used to remove the bands of Cr^{3+} ion. Table 2 shows the Ω_2 and Ω_4 parameters which present similar values for disordered structural systems (heated up to 1000 °C), but the samples treated from 1100 to 1400 °C, the Ω_4 values are higher than Ω_2 parameters. The Ω_2 parameter depends a lot on the lower rank components of the crystal field and dynamic coupling interactions, while the Ω_4 parameter also depends a lot on the corresponding higher components. The samples prepared by Combustion, ceramic and Pechini methods heated at 1400 °C show highest values for the Ω_4 parameters 23.5, 25.7 and 26.4×10^{-20} cm^2, respectively, indicating a high sensitive behavior of the $^5D_0 \rightarrow {}^7F_4$ transition. In the alumina system where $\Omega_4 > \Omega_2$ parameters suggest that the coordination geometry is such that the higher rank components of these interactions have higher values than the lower rank [37].

The values of quantum efficiency ($12 \leqslant \eta \leqslant 32\%$) for the alumina samples are lower when compared to [Eu(TTA)$_3$·

$(DBSO)_2]$ complex ($\eta = 70\%$), where TTA = thenoyltrifluoroacetonate and DBSO = dimethyl sulfoxide [33,34]. Such behavior is in agreement with the balance between the higher values of the non-radiative rate ($A_{nrad} = 1678–4130\ s^{-1}$) and low radiative rate ($A_{rad} = 545–800\ s^{-1}$), as seen in Table 2. However, the europium complex presents high efficiency of intramolecular energy transfer ligand to metal ($A_{nrad} = 420\ s^{-1}$ and $A_{rad} = 980\ s^{-1}$) [34]. This difference can be explained based on O→ Eu^{3+} LMCT states that populate at least partially the ^7F_J ground states of the Eu^{3+} ion, therefore the luminescence is suppressed [7]. The highest value of $\eta = 32\%$ for the doped alumina sample treated at 800 °C is due to low non-radiative rate ($A_{nrad} = 1884\ s^{-1}$) and the highest value of the radiative rate ($A_{rad} = 880\ s^{-1}$).

Based on emission spectra of Al_2O_3:Eu^{3+} phosphor, the (x, y) color coordinates were determined (Table 2). The values of coordinates were around $x = 0.67$ and $y = 0.31$ for the samples heated at different temperatures (400–1400 °C). For the samples annealed at 1100–1400 °C it was also used their deconvoluted emission spectra. The coordinates are located in the red vertex in the CIE (Comission Internacionale l'Eclairage) chromaticity diagram, indicating that the red emission of the Eu3+ into the Al_2O_3 matrix exhibit monochromatic color for all samples [38,39].

4. Conclusions

The Al_2O_3:Eu^{3+} samples annealed up to 700 °C show amorphous character and 800–1000 °C present disordered structural character indicated by the absence of crystallinity peaks in their XRD patterns, suggesting the formation of γ-Al_2O_3. However, the samples heated at 1200–1400 °C show high crystallinity characteristic of the α-Al_2O_3 phase. An abrupt decrease in the BET surface area between 1100 and 1400 °C indicates the phase transition from γ- to α-alumina.

Excitation spectra of Al_2O_3:Eu^{3+} samples prepared by three methods present broad bands arising from Al_2O_3 matrix, to LMCT state of O → Eu^{3+}, and narrow bands assigned to intraconfigurational $4f^6$ transitions of Eu^{3+} ion.

Emission spectra for all Al_2O_3:Eu^{3+} (1%) heated up to 1100 °C exhibit broadened bands for $^5D_0 \rightarrow {}^7F_J$ transitions of Eu^{3+} ion suggesting that this ion is in different symmetry sites indicated by inhomogeneous broadened lines due to disordered structural host lattice (γ-Al_2O_3). However, the presence of narrow lines, assigned to $^5D_0 \rightarrow {}^7F_{0-4}$ transitions of Eu^{3+} ion doped in alumina heated at 1200 and 1400 °C, indicates the transformation of γ- to α-Al_2O_3 phase.

Luminescence decay curves of $^5D_0$ emitter level have a bi-exponential behavior indicating that Eu^{3+} ion is found in a chemical environment with different symmetry sites. The Al_2O_3:Eu^{3+} system prepared by combustion method at 400–1100 °C presents an increase in the Ω_2 intensity parameter values with the increase of annealing temperatures enhancing the covalent character of metal–donor interaction. The values of emission quantum efficiencies (η) of Al_2O_3:Eu^{3+} are higher than those for disordered structural phases. CIE coordinates of samples indicate that the red emissions arising of the Eu^{3+} ion doped in alumina matrix exhibit monochromatic color. Finally, the Eu^{3+} ion acts as a photoluminescent probe for alumina system.

Acknowledgments

The authors thank Conselho Nacional de Desenvolvimento Cientifico e Tecnológico (CNPq), Fundação de Amparo à Pesquisa do Estado de São Paulo (FAPESP), Rede de Nanotecnologia Molecular e de Interfaces (RENAMI) and Instituto do Milênio de Materiais Complexos (IM^2C) for financial support.

References

[1] G. Blasse, B.C. Grabmaier, Luminescent Materials, Springer, Heidelberg, 1994.
[2] R. Reisfeld, C.K. Jorgensen, Lasers and Excited States of Rare Earth, Springer, New York, 1977.
[3] T. Aitasalo, J. Hölsä, H. Jungner, M. Lastusaari, J. Niittykoski, J. Phys. Chem. B 110 (2006) 4589.
[4] C. Feldmann, T. Jüstel, C.R. Ronda, P.J. Schmidt, Adv. Funct. Mat. 13 (2003) 511.
[5] N. Rakov, F.E. Ramos, G. Hirata, M. Xiao, Appl. Phys. Lett. 83 (2003) 272.
[6] J. Hölsä, E. Antic-Fidancev, M. Lastusaari, A. Lupei, J. Solid State Chem. 171 (2003) 282.
[7] C.A. Kodaira, H.F. Brito, O.L. Malta, O.A. Serra, J. Lumin. 101 (2003) 11.
[8] W.M. Fautino, O.L. Malta, E.E.S. Teotônio, H.F. Brito, A.M. Simas, G.F. Sá, J. Chem. Phys. A 110 (2006) 2510.
[9] G.K. Chuah, S. Jaenicke, T.H. Xu, Micropor. Mesopor. Mater. 37 (2000) 345.
[10] J. Sanches-Valente, X. Bokhimi, J.A. Toledo, Appl. Catal. A: General 264 (2004) 175.
[11] A.A. Kaplyanskii, A.B. Kulinkin, A.B. Kutsenko, S.P. Feofilov, R.I. Zakharchenya, T.N. Vasilevskaya, Phys. Solid State 40 (1998) 1310.
[12] O. Ozuna, G.A. Hirata, J. McKittrick, Appl. Phys. Lett. 94 (2004) 1296.
[13] T. Yamamoto, T. Tanaka, T. Matsuyama, T. Funabiki, S. Yoshida, J. Phys. Chem. B 105 (2001) 1908.
[14] G. Hirata, N. Perea, M. Tejeda, J.A. Gonzalez-Ortega, J. McKittrick, Opt. Mater. 27 (2005) 1311.
[15] T. Ishizaka, R. Nozaki, Y. Kurokawa, J. Phys. Chem. Solids 63 (2002) 613.
[16] T. Ishizaka, Y. Kurokawa, J. Appl. Phys. 90 (2001) 243.
[17] J. Wrzyszcz, W. Mińta, D. Hreniak, W. Strek, M. Zawadzki, H. Grabowska, J. Alloy. Compd. 341 (2002) 358.
[18] A. Patra, E. Sominska, S. Ramesh, Y. Koltypin, Z. Zhong, H. Minti, R. Reisfeld, A. Gedanken, J. Phys. Chem. B 103 (1999) 3361.
[19] R. Kudrawiec, J. Misiewicz, L. Bryja, I.S. Molchan, N.V. Gaponenko, J. Alloy. Compd. 341 (2002) 211.
[20] M.U. Pechini, US Patent No. 3330697, 1967.
[21] S. Shikao, W. Jiye, J. Alloy. Compd. 327 (2001) 82.
[22] G.Y. Adachi, K.I. Machida, J. Shiokawa, J. Less-Common Met. 93 (1983) 389.
[23] B.D. Cullity, Elements of X-Ray Diffraction, Addison-Wesley Publishing Company Inc., Reading, Massachusetts, 1967.
[24] K. Nakamoto, Infrared and Raman Spectra of Inorganic and Coordination Compounds, Willey-Interscience Publication, 1986.
[25] M.T. Hernández, M. González, J. Eur. Ceram. Soc. 22 (2002) 2861.

[26] S. Desset, O. Spalla, P. Lixon, B. Cabane, Colloids Surface A: Phys. Eng. Aspects 196 (2002) 1.
[27] Q. Dai, G.N. Robinson, A. Freedman, J. Phys. Chem. B 101 (1997) 4940.
[28] C. Laberty-Robert, F. Ansart, C. Deloget, M. Gaudon, A. Rousset, Mater. Res. Bull. 36 (2001) 2083.
[29] S.T. Aruna, K.S. Rajam, Mater. Res. Bull. 39 (2004) 157.
[30] Y. Sarikaya, K. Ada, T. Alemdaroglu, I. Bozdogan, J. Eur. Ceram. Soc. 22 (2002) 1905.
[31] S. Cava, S.M. Tebcherani, S.A. Pianaro, C.A. Paskocimas, E. Longo, J.A. Varela, Mater. Chem. Phys. 97 (2006) 102.
[32] R.G. Burns, Mineralogical Applications of Crystal Field Theory, Cambridge University Press, 1993.
[33] O.L. Malta, H.F. Brito, J.F.S. Menezes, F.R.G. Silva, S. Alves Jr., F.S. Farias Jr., A.V.M. de Andrade, J. Lumin. 75 (1997) 255.
[34] G.F. Sá, O.L. Malta, C.M. Donegá, A.M. Simas, R.L. Longo, P.A. Santa-Cruz, E.F. da Silva Jr., Coord. Chem. Rev. 196 (2000) 165.
[35] G.L. Baugis, H.F. Brito, W. Oliveira, F.R. Castro, E. F Souza-Aguiar, Micropor. Mesopor. Mater. 49 (2001) 179.
[36] W.T. Carnall, H. Crosswhite, H.M., Crosswhite – Energy Structure and Transition Probabilities of the Trivalent Lanthanides in LaF_3, Argonne National Laboratory Report, unnumbered, 1977.
[37] O.L. Malta, S.J.L. Ribeiro, M. Faucher, P. Porcher, J. Chem. Phys. Solids 52 (1991) 587.
[38] L.D. Carlos, Y. Messaddeq, H.F. Brito, R.A.S. Ferreira, V.Z. Bermudez, S.J.L. Ribeiro, Adv. Mater. 12 (2000) 594.
[39] P.A. Santa-Cruz, F.S. Teles, Spectra Lux Software v.1.0, Ponto Quántico Nanodispositivos – RENAMI, 2003.